

Neighborhood-Adaptive Generalized Linear Graph Embedding with Latent Pattern Mining

Shuai Peng, Liangchen Hu, Wensheng Zhang, Biao Jie, and Yonglong Luo

Abstract—Graph embedding has been widely applied in areas such as network analysis, social network mining, recommendation systems, and bioinformatics. However, current graph construction methods often require the prior definition of neighborhood size, limiting the effective revelation of potential structural correlations in the data. Additionally, graph embedding methods using linear projection heavily rely on a singular pattern mining approach, resulting in relative weaknesses in adapting to different scenarios. To address these challenges, we propose a novel model, Neighborhood-Adaptive Generalized Linear Graph Embedding (NGLGE), grounded in latent pattern mining. This model introduces an adaptive graph learning method tailored to the neighborhood, effectively revealing intrinsic data correlations. Simultaneously, leveraging a reconstructed low-rank representation and imposing $\ell_{2,0}$ norm constraint on the projection matrix allows for flexible exploration of additional pattern information. Besides, an efficient iterative solving algorithm is derived for the proposed model. Comparative evaluations on datasets from diverse scenarios demonstrate the superior performance of our model compared to state-of-the-art methods.

Index Terms—Graph embedding, adaptive neighborhood, low-rank representation, row sparsity

I. INTRODUCTION

AMIDST the challenges of processing high-dimensional data in the contemporary landscape, graph embedding technology emerges as a potent tool [1], [2]. It effectively maps intricate graph structures into a low-dimensional vector space, providing a fresh avenue for data analysis. Graph embedding transcends mere dimensionality reduction [3], [4], emphasizing the preservation of the original data's topological structure and relationships within the reduced space. This ensures that the similarity between nodes persists in the new representation. Notably, among these methods, graph embedding approaches that utilize linear projection for out-of-sample extension are particularly intriguing [5], [6], [7], [8].

Currently, graph construction methods can be broadly categorized into two main classes: predefined methods [5], [6],

This work was supported in part by the Natural Science Project in Universities of Anhui Province under Grant 2022AH040028, and in part by the National Natural Science Foundation of China under Grant 62306010, Grant 62272006, and Grant 61976006, and in part by the Anhui Normal University High-Peak and Incentive Discipline Construction Project under Grant 2023GFXK171. (Corresponding author: Liangchen Hu.)

Shuai Peng, Liangchen Hu, Biao Jie, and Yonglong Luo are with the School of Computer and Information, Anhui Normal University, Wuhu 241002, China, and also with the Anhui Provincial Key Laboratory of Industrial Intelligent Data Security, Wuhu 241002, China (e-mail: pengshuai@ahnu.edu.cn; cslc.hu@ahnu.edu.cn; jbiao@ahnu.edu.cn; ylluo@ustc.edu.cn).

Wensheng Zhang is with the Institute of Automation, State Key Laboratory of Multimodal Artificial Intelligence Systems, Chinese Academy of Sciences, Beijing 100190, China, and also with the School of Artificial Intelligence, University of Chinese Academy of Sciences, Beijing 100049, China (e-mail: zhangwenshengia@hotmail.com).

[7], [9] and dynamically adaptive methods tailored to the data. The latter encompasses four subcategories [10], namely regularization penalty [11], [12], [13], power weighting [14], [15], norm-induced self-weighting [16], and non-negative self-representation [17], [18]. However, graph embedding methods primarily rely on a single pattern mining approach, typically maintaining only the similarity between nodes in the graph. Therefore only preserving a kind of structure usually cannot obtain the consistent good performance for different datasets.

In recent years, the low-rank-based feature extraction method has received a lot of attention owing to its robustness to noise and good performance in uncovering the intrinsic global structure of data [19], [20], [21], [22]. However, it is a pity that the original low-rank representation (LRR) [23] cannot deal with new samples which are not involved in the training stage. To address this issue, Latent LRR (LatLRR) takes the hidden data into account and learns a low-rank projection to extract salient features for unsupervised classification [24]. Double LRR (DLRR) is also proposed for projection learning, in which the principle component recovery and salient feature extraction terms of LatLRR are integrated into a term [25]. Although the above LRR-based methods have shown their robustness in feature extraction, they lose the ability of dimensionality reduction since the obtained projection has the same dimension with the original data. But there are many methods have been proposed to tackle this problem subsequently [26], [27], [28].

To integrate the low-rank property, some graph embedding methods were extended for robust feature extraction, such as low-rank preserving projection (LRPP) [17], low-rank preserving embedding (LRPE) [29], low-rank linear embedding (LRLE) [30] and low-rank preserving projection via graph regularized reconstruction (LRPP_GRR) [9]. The above-mentioned methods tend to utilize multiple pattern in mining intrinsic structure of the data. However, in this field, there are still some core issues. Firstly, current graph construction methods often require the predefined specification of neighborhood size (including adaptive graph learning method), limiting the effective revelation of potential structural relationships in the data. This rigid neighborhood definition may fail to capture the diversity and complexity present in real-world data. Secondly, the above feature extraction methods do not have strong interpretability since the extracted features are the linear combinations of all the original features. Thus it is difficult to interpret which features are the most important for the given task. In other words, all original high-dimensional features include outliers and noises are regarded as useful features in these methods. This is contradictory with the purpose

of the feature extraction which aims to extract useful and discriminative features.

To address these challenges, we will focus on the linear graph embedding and strive to enhance graph construction methods, improve their ability to reveal the latent structure of the data, and conduct in-depth research into more flexible and diverse graph embedding techniques. By delving into dynamic adaptive graph construction methods, we aim to enhance the adaptability of graph embedding techniques across diverse scenarios and complex data structures. To achieve the interpretability of projection, the $\ell_{2,0}$ norm is introduced to constrain the projection matrix owing to its column-sparsity property. In this way, NGLGE can select the most important features from the original data for feature extraction. This research provides new insights into high-dimensional data dimensionality reduction, driving the further development of graph embedding technologies in practical applications.

In brief, our study has the following key contributions:

- We presents a novel unsupervised projection learning approach which utilize low-rank property to preserve global and learn a adaptive weight graph to describe local structures. In addition, feature selection also be integrate to our model to filtered redundancy feature.
- To solve the proposed model, we developed an efficient iterative algorithm and conducted experiments on various publicly available datasets in different scenarios, demonstrating that our algorithm achieves excellent performance in dimensionality reduction.
- Specially, different with previous works, we develop a novel but simple algorithm to optimize the Neighborhood-Adaptive graph which can effectively and exactly find the analytical global optimal solution, then mathematical proofs were subsequently given.

The remainder of this paper is structured as follows. Section II provides some notations in our writing and offers a concise overview of related approaches in the field. Next, in Section III, we present our novel model, discuss the optimization process, and analyze its computational complexity. The experimental setup and results are detailed in Section IV. Finally, we conclude the paper in Section V.

II. RELATED WORK

A. Notations and definitions

Assuming a data matrix $X = [X_1, X_2, \dots, X_c] = [x_1, x_2, \dots, x_n] \in \mathbb{R}^{d \times n}$ consisting of n samples in a d -dimensional space, where each X_i represents a sub-matrix belonging to the i -th class. For any vector $x = [x_1, x_2, \dots, x_n]$, the ℓ_2 -norm is defined as $\|x\|_2 = \sqrt{\sum_{i=1}^n x_i^2}$ and the ℓ_0 -norm is defined as the number of non-zero entries. For any matrix $X \in \mathbb{R}^{d \times n}$, the Frobenius norm is defined as $\|X\|_F^2 = \sum_{j=1}^n \sum_{i=1}^d x_{ij}^2$, the $\ell_{2,1}$ -norm is defined as $\|X\|_{2,1} = \sum_{j=1}^n \sqrt{\sum_{i=1}^d x_{ij}^2}$, the $\ell_{2,0}$ -norm is defined as $\|X\|_{2,0} = \|\eta\|_0$, where the j -th entry of vector η is the ℓ_2 norm of the j -th column vector of X . $\|X\|_*$ represents the nuclear norm of X which is the sum of singular values.

B. Adaptive neighbors learning

To overcome the disadvantage of the similarity measurement and projection learning are often conducted in two separated steps, Nie et al. [11] proposed a adaptive neighbors learning model. The goal is to find an optimal subspace on which the adaptive neighboring is performed. Denote the total scatter matrix by $S_t = X H X^T$, where H is the centering matrix defined by $H = I - \frac{1}{n} \mathbf{1} \mathbf{1}^T$ and then, the model is as follows:

$$\begin{aligned} \min_{Q, S} & \sum_{i=1}^n \sum_{j=1}^n (\|Qx_i - Qx_j\|_2^2 s_{ij} + \gamma s_{ij}^2) \\ \text{s.t. } & QS_t Q^T = I, \quad S \geq 0, \quad S\mathbf{1} = \mathbf{1} \end{aligned} \quad (1)$$

where $QS_t Q^T = I$ can result in a statistically uncorrelated subspace. Note that the parameter γ is not predetermined but determined during the optimization process by specifying the number of neighbors.

C. Efficient sparse feature selection

In [31], Pang et al. proposed a novel algorithm which can solve the original $\ell_{2,0}$ -norm constrained sparse based feature selection problem directly instead of its approximate problem. their optimization function can be formulated as follows:

$$\begin{aligned} \min_{Q, \mathbf{b}} & \|QX + \mathbf{1}\mathbf{b} - Y\|_F^2 \\ \text{s.t. } & \|Q\|_{2,0} = \alpha \end{aligned} \quad (2)$$

where \mathbf{b} is bias and Y is regression label. The $\ell_{2,0}$ -norm constraint of Q makes the number of its non-zero columns be equal to α , which ensures the sparsity of the model and makes the model have the ability to select features. In this article, we use the same strategy to optimize our model.

III. METHODOLOGY

In this section, we present a method named NGLGE to learn the optimal projection for unsupervised classification. To solve (7) effectively, we develop an efficient ADMM-based optimization algorithm. Additionally, analysis of the computational complexity involved in the algorithm is also presented.

A. Proposed method

Linearly projecting graph nodes into a low-dimensional space while minimizing dissimilarity between pairs of nodes in the embedded space to preserve the local neighborhood of nodes in the original space. The objective is defined as follows

$$\min_Q \sum_{i=1}^n \sum_{j=1}^n \|Qx_i - Qx_j\|_2^2 s_{ij} \quad (3)$$

where the projection matrix $Q \in \mathbb{R}^{m \times d}$ ($m < d$) transforms x_i into a lower-dimensional space, and s_{ij} denotes the affinity between x_i and x_j . In model (3), relying solely on the preservation of the adjacency of nodes in the graph to ensure the exploration of latent patterns in the data is overly simplistic.

In [25], discriminative structural information is adeptly extracted from observed data through the concurrent recovery of information from both row and column spaces, as follows

$$\min_{Z, L, E} \|Z\|_* + \|L\|_* + \lambda \|E\|_1 \quad \text{s.t. } X = LXZ + E \quad (4)$$

where $L \in \mathbb{R}^{d \times d}$ and $Z \in \mathbb{R}^{n \times n}$ are two low-rank representation matrices, E contains noise or errors, and λ is a regularization parameter. To enrich the disclosure of latent patterns in the data, we hereby examine the correlation between the original X and the intrinsic LXZ below

$$\min_{Z, L} \sum_{i=1}^n \sum_{j=1}^n \|x_i - LXz_j\|_2^2 s_{ij} + \lambda_1 \|L\|_* + \lambda_2 \|Z\|_* \quad (5)$$

where λ_1 and λ_2 are two regularization parameters. Considering L as a low-rank matrix, it can be expressed as $L = PQ$, where $P \in \mathbb{R}^{d \times m}$, indicating that $\text{rank}(L) \leq m < d$. With the constraint $P^T P = I$, (5) can be expressed as

$$\begin{aligned} \min_{P, Q, Z} & \sum_{i=1}^n \sum_{j=1}^n \|x_i - PQXz_j\|_2^2 s_{ij} + \lambda_1 \|Q\|_F^2 + \lambda_2 \|Z\|_* \\ \text{s.t. } & P^T P = I, \|Q\|_{2,0} = \alpha \end{aligned} \quad (6)$$

where $\|Q\|_{2,0} = \alpha$ compels the number of non-zero columns in the projection matrix Q to be equal to α , endowing the model with feature selection capability and enhancing the exploration of latent patterns within the data.

Moreover, in the presence of noise-contaminated data, the pre-constructed graph fails to precisely capture the affinity within the data. In light of this, we make S adaptively to learn probabilistic neighborhood graph, as detailed below

$$\begin{aligned} \min_{P, Q, Z, S} & \sum_{i=1}^n \sum_{j=1}^n \|x_i - PQXz_j\|_2^2 s_{ij} + \lambda_1 \|Q\|_F^2 \\ & + \lambda_2 \|Z\|_* + \lambda_3 \|S\|_F^2 \\ \text{s.t. } & P^T P = I, S \geq 0, S^T \mathbf{1} = \mathbf{1}, \|Q\|_{2,0} = \alpha \end{aligned} \quad (7)$$

B. Optimization

In this section, we address the problem presented in (7) using the alternating direction method of multipliers (ADMM) framework [32]. A detailed convergence analysis of ADMM for nonconvex problems is available in [33]. To facilitate the optimization process, we introduce an auxiliary variable B and impose a constraint $Z = B$ to achieve separability in (7). Thus, by relaxing the original problem, we can reformulate (7) as follows

$$\begin{aligned} \min_{P, Q, Z, S} & \sum_{i=1}^n \sum_{j=1}^n \|x_i - PQXz_j\|_2^2 s_{ij} + \lambda_1 \|Q\|_F^2 \\ & + \lambda_2 \|B\|_* + \lambda_3 \|S\|_F^2 \\ \text{s.t. } & P^T P = I, S \geq 0, S^T \mathbf{1} = \mathbf{1}, \|Q\|_{2,0} = \alpha, Z = B \end{aligned} \quad (8)$$

For convenience of taking derivative, we rewrite the first and second terms in trace form.

$$\begin{aligned} \min_{P, Q, Z, S} & \text{Tr}(X^T X D_1) - 2\text{Tr}(X^T P Q X Z S^T) \\ & + \text{Tr}(Z^T X^T Q^T Q X Z D_2) + \lambda_1 \text{Tr}(Q^T Q) \\ & + \lambda_2 \|B\|_* + \lambda_3 \|S\|_F^2 \\ \text{s.t. } & P^T P = I, S \geq 0, S^T \mathbf{1} = \mathbf{1}, \|Q\|_{2,0} = \alpha, Z = B \end{aligned} \quad (9)$$

where $D_1 = \text{diag}(\sum_{j=1}^n s_{1j}, \sum_{j=1}^n s_{2j}, \dots, \sum_{j=1}^n s_{nj})$ and $D_2 = \text{diag}(\sum_{i=1}^n s_{i1}, \sum_{i=1}^n s_{i2}, \dots, \sum_{i=1}^n s_{in})$.

Then, the augmented Lagrangian function of (9) is defined by

$$\begin{aligned} \mathcal{L}(P, Q, Z, S, B) &= \text{Tr}(X^T X D_1) - 2\text{Tr}(X^T P Q X Z S^T) \\ &+ \text{Tr}(Z^T X^T Q^T Q X Z D_2) + \lambda_1 \text{Tr}(Q^T Q) \\ &+ \lambda_2 \|B\|_* + \lambda_3 \|S\|_F^2 + \langle C, Z - B \rangle \\ &+ \frac{\mu}{2} \|Z - B\|_F^2 \\ \text{s.t. } & P^T P = I, S \geq 0, S^T \mathbf{1} = \mathbf{1}, \|Q\|_{2,0} = \alpha \end{aligned} \quad (10)$$

where $\langle A, B \rangle = \text{trace}(A^T B)$. Note that D_2 is a identity matrix, so we ignore it later.

Update Z : Given fixed P, Q, S and B , the subproblem for solving Z is as follows

$$\begin{aligned} \min_Z & \text{Tr}(Z^T X^T Q^T Q X Z) - 2\text{Tr}(X^T P Q X Z S^T) \\ & + \langle C, Z - B \rangle + \frac{\mu}{2} \|Z - B\|_F^2 \end{aligned} \quad (11)$$

Let $\partial \mathcal{L}(Z)/\partial Z = 0$, we have

$$(2X^T Q^T Q X + \mu I)Z = 2X^T Q^T P^T X S + \mu B - C \quad (12)$$

Then Z is updated by

$$Z = (2X^T Q^T Q X + \mu I)^{-1}(2X^T Q^T P^T X S + \mu B - C) \quad (13)$$

Update B : Given fixed Z , the subproblem concerning B is as follows

$$\min_B \lambda_2 \|B\|_* + \frac{\mu}{2} \|Z - B\|_F^2 + \frac{C}{\mu} \quad (14)$$

Then B is obtained by using the singular value thresholding (SVT) shrinkage operator [28] as follows

$$B = \Theta_{\lambda_2/\mu} \left(Z + \frac{C}{\mu} \right) \quad (15)$$

where Θ is the SVT shrinkage operator.

Update Q : Given fixed P, Z and S , the problem w.r.t. Q becomes

$$\begin{aligned} \min_Q & \text{Tr}(Z^T X^T Q^T Q X Z) - 2\text{Tr}(X^T P Q X Z S^T) \\ & + \lambda_1 \text{Tr}(Q^T Q) \\ \text{s.t. } & \|Q\|_{2,0} = \alpha \end{aligned} \quad (16)$$

where $m \leq \alpha \leq d$. Motivated by [31], we conduct full rank decomposition on Q , i.e.,

$$Q = VU \quad (17)$$

where $V \in \mathbb{R}^{m \times \alpha}$ is composed by all non-zero columns of Q and $U \in \mathbb{R}^{\alpha \times d}$ is a selection matrix. It is worth noticing that the full rank decomposition is not unique. Here, for the purpose of feature selection, we impose constraints on U

$$U = [\mathbf{u}_{s(1)}; \mathbf{u}_{s(2)}; \dots; \mathbf{u}_{s(\alpha)}] \quad (18)$$

where the vector \mathbf{s} is a permutation of $\{1, 2, \dots, d\}$ and \mathbf{u}_i is the i -th row of identity matrix $I \in \mathbb{R}^{d \times d}$. By replacing Q in problem (16) with (17), we have

$$\begin{aligned} \min_{U \in \text{selec}, V} & \text{Tr}[VU(XZZ^TX^T + \lambda_1 I)U^TV^T] \\ & - 2\text{Tr}(VUXZS^TX^TP) \end{aligned} \quad (19)$$

Then, after taking derivative of problem (19) w.r.t. V and assigning this value to zero, we get

$$V = P^T XSZ^T X^T U^T [U(XZZ^TX^T + \lambda_1 I)U^T]^{-1} \quad (20)$$

Then, substituting (20) into (19) and denoting $F = P^T XSZ^T X^T$, $G = XZZ^TX^T + \lambda_1 I$, we have

$$\begin{aligned} \min_{U \in \text{selec}} & \text{Tr}[FU^T(UGU^T)^{-1}UF^T] \\ & - 2\text{Tr}[FU^T(UGU^T)^{-1}UF^T] \end{aligned} \quad (21)$$

Therefore, problem (21) becomes

$$\max_{U \in \text{selec}} \text{Tr}[(UGU^T)^{-1}UF^T FU^T] \quad (22)$$

To maximize problem (22), we select the largest α diagonal elements of $(G^{-1})(F^T F)$ and denote the row (or column) indices vector of the largest α diagonal elements as $\mathbf{q} = \{q_1, q_2, \dots, q_\alpha\}$, where $q_\alpha \in \{1, 2, \dots, d\}$. Then, $U_{iq_i} = 1, i = 1, 2, \dots, \alpha$ while other element is zero [34].

Update P : Given fixed Q , Z and S , update P by solving the following maximization problem:

$$\begin{aligned} \max_P & \text{Tr}(X^T P Q X Z S^T) \\ \text{s.t. } & P^T P = I \end{aligned} \quad (23)$$

The problem (23) is a orthogonal procrustes problem (OPP) problem [35] which can be simply solved by singular value decomposition (SVD). We compute the thin SVD of $XSZ^T X^T Q^T$, i.e.,

$$XSZ^T X^T Q^T = U_{d \times m} \Sigma V_{m \times m}^T \quad (24)$$

where $m \leq d$, then, we get

$$P = U V^T \quad (25)$$

where U and V consist of the left-singular vectors and right-singular vectors of $XSZ^T X^T Q^T$, respectively.

Update S : Given fixed P , Q and Z , the subproblem for updating S is

$$\begin{aligned} \min_S & \sum_{i=1}^n \sum_{j=1}^n a_{ij} s_{ij} + \lambda_3 \|S\|_F^2 \\ \text{s.t. } & S \geq 0, S^T \mathbf{1} = \mathbf{1} \end{aligned} \quad (26)$$

where $a_{ij} = \|x_i - PQXz_j\|_2^2$. We break down the problem (26) in n independent sub-problems

$$\begin{aligned} \min_{\mathbf{s}_j} & \sum_{i=1}^n a_{ij} s_{ij} + \lambda_3 \|\mathbf{s}_j\|_2^2 \\ \text{s.t. } & \mathbf{s}_j \geq 0, \sum_{i=1}^n s_{ij} = 1 \end{aligned} \quad (27)$$

To optimize this problem, Nie et al. [11] proposed a method which has since been frequently adopted. But in that way, the all training sample have same number of neighbors, which may lead to incorrect connections between samples. To fix this problem, we develop a new algorithm which can effectively and exactly find the analytical global optimal solution. We discuss the new algorithm in more detail later and give mathematical proof subsequently.

Update C and μ : C and μ are respectively updated by

$$\begin{aligned} C &= C + \mu(Z - B) \\ \mu &= \min(\rho\mu, \mu_{max}) \end{aligned} \quad (28)$$

The detailed optimization procedure of (7) is presented in Algorithm 1.

Algorithm 1 Solving problem (7) via ADMM.

Input: Training samples $X \in \mathbb{R}^{d \times n}$, hyper-parameters λ_1 , λ_2 , λ_3 and projected dimension m .

Output: Discriminative projection matrix Q .

- 1: **Initialize** $P = \arg \max_{P^T P = I} \text{Tr}(P^T \Sigma P)$, where Σ is the data covariance; $Q = P^T$, $Z = B = 0$, $s_{ij} = 1/k$ if $x_i \in N_k(x_j)$, $s_{ij} = 0$ otherwise; $C = 0$, $\mu = 0.1$, $\rho = 1.1$, $\mu_{max} = 10^8$, $\epsilon = 10^{-6}$ and $maxIter = 60$.
- 2: **repeat**
- 3: Update Z using (13).
- 4: Update B using (15).
- 5: Update Q using (17).
- 6: Update P using (25).
- 7: Update S using (32).
- 8: Update C and μ using (28).
- 9: **until** the following convergence conditions are fulfilled

$$\|Z - B\|_\infty \leq \epsilon$$

or iteration reaches $maxIter$.

C. Optimization algorithm for updating S

For simple of notation, we discuss the following generalized problem:

$$\begin{aligned} \min_{\mathbf{s}} & \sum_{i=1}^n a_i s_i + \gamma \|\mathbf{s}\|_2^2 \\ \text{s.t. } & \mathbf{s} \geq 0, \sum_{i=1}^n s_i = 1 \end{aligned} \quad (29)$$

where \mathbf{a} and \mathbf{s} are vectors with n elements. For convenience to characterize the algorithm of this problem, we denote

$$S^t = \{i \mid a_i < c^{t-1}\}, \quad t = 1, 2, \dots \quad (30)$$

$$c^t = \frac{\sum_{i \in S^t} a_i}{k_t} + \frac{2\gamma}{k_t}, \quad t = 0, 1, \dots \quad (31)$$

where S^t is a index set, k_t is number of elements in S^t . We first let $S^0 = \{1, 2, \dots, n\}$, then all variables will be defined recursively. Then, we only need to find the t that makes $c^t = c^{t-1}$ (or $k^t = k^{t-1}$).

In the worst case, it is only necessary to compute up to c^n for us to find $c^t = c^{t-1}$. If the t has been found, then

$$s_i = \begin{cases} \frac{\sum_{i \in S^t} a_i}{2\gamma k_t} - \frac{a_i}{2\gamma} + \frac{1}{k_t}, & i \in S^t \\ 0, & \text{otherwise} \end{cases} \quad (32)$$

Next, we discuss why s obtained by (32) is optimal.

Lemma 1: The sequence c^t , $t = 0, 1, \dots$, is nonincreasing.

Proof: We only prove that $c^0 \geq c^1$ here, it is similar to prove $c^t \geq c^{t+1}$ for any t . Supposing that $a_1, a_2, \dots, a_k, a_{k+1}, \dots, a_n$ is sorted in ascending order, then, $c^0 = \frac{\sum_{i=1}^n a_i}{n} + \frac{2\gamma}{n}$. Without loss of generality, assuming that $a_1, \dots, a_k < c^0$ and $a_{k+1}, \dots, a_n \geq c^0$. Then, $c^1 = \frac{\sum_{i=1}^k a_i}{k} + \frac{2\gamma}{k}$. We need to prove that $c^0 \geq c^1$, e.g.:

$$\frac{\sum_{i=1}^n a_i}{n} + \frac{2\gamma}{n} \geq \frac{\sum_{i=1}^k a_i}{k} + \frac{2\gamma}{k} \quad (33)$$

The inequality is not obvious, because from left to right, the value of the first term decreases while the value of the second term increases. But we can prove this inequality from known conditions. From $a_{k+1}, \dots, a_n > c^0$, we have:

$$\frac{\sum_{i=k+1}^n a_i}{n-k} \geq \frac{\sum_{i=1}^n a_i}{n} + \frac{2\gamma}{n} \quad (34)$$

The left side of (34) is the mean value of a_{k+1}, \dots, a_n . Using some simple algebra, yields:

$$n \sum_{i=k+1}^n a_i \geq (n-k) \left(\sum_{i=1}^n a_i + 2\gamma \right) \quad (35)$$

$$n \sum_{i=1}^k a_i + n \sum_{i=k+1}^n a_i \geq n \left(\sum_{i=1}^n a_i + 2\gamma \right) - k \left(\sum_{i=1}^n a_i + 2\gamma \right) + n \sum_{i=1}^k a_i \quad (36)$$

$$k \sum_{i=1}^n a_i + 2k\gamma \geq n \sum_{i=1}^k a_i + 2n\gamma \quad (37)$$

$$\frac{\sum_{i=1}^n a_i}{n} + \frac{2\gamma}{n} \geq \frac{\sum_{i=1}^k a_i}{k} + \frac{2\gamma}{k} \quad (38)$$

where (38) is exactly identical to (33) which is required to be proven. ■

Theorem 1: Computing s by (32) yields the optimal solution for problem (29).

Proof: The KKT conditions for problem (29) are as follows

$$\begin{aligned} s_i &\geq 0, \quad i = 1, \dots, n \\ \sum_{i=1}^n s_i &= 1, \\ \lambda_i &\geq 0, \quad i = 1, \dots, n \\ \lambda_i s_i &= 0, \quad i = 1, \dots, n \\ \mathbf{a} + 2\gamma \mathbf{s} - \lambda + \nu \mathbf{1} &= 0, \end{aligned} \quad (39)$$

where ν is a scalar and $\lambda, \mathbf{1} \in \mathbb{R}^n$. Because problem (29) is convex problem and the objective function is strongly convex, if we can find s together with (λ, ν) that satisfy the KKT conditions, s is optimal [36].

Because $a_i < c^t$, by (32), the first and second KKT conditions can be satisfied. Then calculate ν . For those $s_i > 0$, λ_i is 0. By the last KKT condition, we have:

$$2\gamma s_i = -a_i - \nu \quad (40)$$

Sum both sides of the equation for nonzero s_i and solve ν

$$\nu = -\frac{\sum_{i \in S^t} a_i}{k_t} - \frac{2\gamma}{k_t} \quad (41)$$

Finally, we need to find appropriate λ_i corresponding to zero s_i . Those λ_i must satisfy the third and last KKT conditions:

$$\lambda_i \geq 0 \quad (42)$$

$$a_i - \lambda_i = \frac{\sum_{i \in S^t} a_i}{k_t} + \frac{2\gamma}{k_t} \quad (43)$$

Note that the right side of (43) is c^t while $c^t \leq c^{t-1} \leq c^{t-2} \leq \dots \leq c^0$. Recall that all a_i corresponding to zero s_i greater than or equal to one of $\{c^0, c^1, \dots, c^t\}$, thus greater than or equal to the c^t .

Overall, we can find λ_i that satisfies both (42) and (43). So s is optimal because there are (λ, ν) that, together with s , satisfy the KKT conditions. ■

D. Complexity analyses

The computational complexity of the model mainly depends on the complexity of Algorithm 1 in which the main time-consuming operations are solving the inverse of square matrix and performing SVD.

Next, we discuss the main computational complexity of each step. To update Z , the main time consuming step is to compute $(2X^T Q^T Q X + \mu I)^{-1}$, where the computational complexity is about $O(n^3)$. To update B , the most demanding computation is the SVD computation of matrix $(Z + C/\mu)$, and thus the computational complexity is $O(n^3)$. To update Q , the main time consuming step is to compute $(UGU^T)^{-1}$, in which the computational complexity is about $O(d^3)$. When updating P , the computational complexity is dominated by the singular value decomposition (SVD) computation of $X S Z^T X^T Q^T$, which has a complexity of $O(m^3)$ [28]. The optimization of the S is relatively simple, so the computational cost of solving S can be ignored. Overall, Algorithm 1 has a total computational complexity of $O(\tau(n^3 + d^3 + m^3))$, where τ denotes the number of iterations. In practical scenarios, it is common to have $d \ll n$ and a small value of m . Hence, the total computational complexity of the model can be loosely approximated as $O(\tau n^3)$.

IV. EXPERIMENTS

In this section, we evaluate the effectiveness of the proposed method on six widely-used public datasets collected from diverse scenarios. To ensure a convincing comparison, the proposed method is compared with some state-of-the-art methods including LPP [5], NPE [37], OLPP [6], PCAN [11], SOGFS [38], RJSE [39], RDR [40], LRLE [30], LRPP_GRR [9], FSP [41], LRAGE [42].

A. Databases

Here, six distinctive and widely-used databases are employed to demonstrate the validity of our algorithm.

EYaleB [43] - The Extended Yale B database consists of a total of 2414 face images captured from 38 volunteers. Each volunteer provided 59-64 images with different illuminations. Moreover, half of the images per person contain varying degrees of shadows. In the experiments, each sample was resized to 32×32 pixels.

YTC [44] - The YouTube-Celebrities (YTC) dataset consists of 1910 video clips featuring 47 celebrities sourced from YouTube. These videos are obtained from real-life scenarios, exhibiting significant variations in facial expressions, appearances and poses, as well as containing noise, misalignments, poor quality, and occlusions. Each of the 1910 video clips contains 8-400 frames, and each celebrity is represented by more than 1000 images. For our experiments, 200 images of each celebrity are randomly selected as the experimental data (i.e., 9400 images in total). The face images are uniformly resized to 30×30 pixels.

Binalpha¹ - This database consists of 1404 samples distributed among 36 classes. Each sample is represented by a binary image of 20×16 pixels. The database encompasses not only digits ranging from “0” to “9” but also capital letters from “A” to “Z”. Notably, There are several pairs of easily confused letters and numbers such as “0” and “O”, “2” and “Z”, “5” and “S”, “6” and “G”, “8” and “B”, thus posing a challenge to classification.

USPS [45] - The USPS dataset is a collection of handwritten digital images comprising 10 classes from “0” to “9”. The dataset contains a total of 9289 images, with each class consisting of varying numbers of samples ranging from 708 to 1553 images. To facilitate analysis, all images have been resized to 16×16 pixel gray images, so the original dimensional of samples is 256.

ETH80 [46] - The ETH80 dataset comprises visual object images belonging to 8 different categories including apples, cars, cows, cups, dogs, horses, pears and tomatoes. For each category, there are 10 object instances, and images of each object instance were captured from 41 different viewpoints. In our experiment, we resized the gray images to 20×20 pixels and converted them to 400-dimensional vectors.

15-Scene [47] - The 15-Scene database totally includes 4485 images from 15 natural scene categories, which is commonly used in the evaluation of scene recognition. A variety of scenes can be found in the database, including Bedroom, Coast, Forest, Highway, Industrial, InsideCity, Kitchen, LivingRoom, Mountain, Office, OpenCountry, Store, Street, Suburb and TallBuilding, with about 210 to 410 samples in each category. Instead of using the original features, we employ the spatial pyramid features presented in [48] for recognition, where each sample has 3000 dimensions.

B. Experimental setup

In our experiments, the nearest neighbor (1-NN) classifier is employed to classify samples using the Euclidean distance.

¹<https://cs.nyu.edu/~roweis/data.html>

Parameters for methods are fine-tuned or set following authors’ recommendations, except for neighbor size, which is uniformly set to the number of training samples in each class. For our method, we preset $s_{ij} = 0$ if $x_i \notin N_k(x_j)$ where k is neighbor size, then optimize the remaining s_{ij} . For LPP, OLPP, RDR, LRLE, LRPP_GRR and FSP the pre-constructed graph is weighted by 0-1 while others don’t need to define the graph in advance. To mitigate the effects of randomness, we implement all algorithms in the comparison experiments 10 times and report the mean recognition rates. For each experiment, we randomly select a number of samples for each class as the training data (#Tr), while using the remaining samples as the test data. To improve the computational efficiency, we first apply PCA to reduce the dimensions of the data by preserving 98% of the energy across all databases except dimension of 15-Scene is reduced to 198. Preserving 98% of the energy means selecting only the first k vectors corresponding to the k largest eigenvalues that satisfy $\sum_{i=1}^k \lambda_i / \sum_{i=1}^n \lambda_i = 0.98$, where λ_i denotes the i -th largest eigenvalue of the covariance matrix of the original data and n is the total number of eigenvalues. These selected vectors are used to form the projection matrix of PCA for dimensionality reduction and then perform sample normalization e.g. $x_i = x_i / \|x_i\|_2$. Before training the (1-NN) classifier, We also normalize both training and test samples to get recognition rate.

C. Experiment result and analysis

The results of each algorithm across diverse datasets are summarized in Table I leading to the following conclusions:

1) LRPP_GRR and our method excel in classification accuracy on EYaleB and YTC datasets, surpassing other methods. it implies that combining the graph regularization for local structure and low-rank representation for global structure proves to be beneficial.

2) Our method outperforms LRPP_GRR and others on Binalpha and USPS datasets, which may implies that neighborhood-adaptive graph learning and $\ell_{2,0}$ -norm feature selection show effectiveness in reducing inter-class margins and filtering redundant features.

3) Form the experiment results of ETH80 dataset, our method competes well, particularly with 20, 30, or 40 training samples per class. LRLE excels with 10 samples per class, indicating our method’s ability to leverage discriminative information with ample training samples.

4) On the 15-Scene dataset, our method consistently outperforms others. Notably, achieving over 90% accuracy with a small training set demonstrates strong generalization.

D. Parameters sensitivity study

The classification performance of model (7) can be influenced by four tunable parameters, namely λ_1 , λ_2 , λ_3 , and α . However, adaptively selecting suitable parameters remains an open problem for various tasks, and no efficient solution has been proposed thus far. To simplify the process of discovering the optimum parameters, we fix α to $\max(m, [0.9d])$, e.g., selecting 90% original feature. In our experiments, we observed minimal relevance of λ_3 to other

TABLE I
MEAN RECOGNITION ACCURACIES AND STANDARD DEVIATIONS (%) OF VARIOUS ALGORITHMS ON SIX DIFFERENT DATABASES

Dataset	#Tr	LPP	NPE	OLPP	PCAN	SOGFS	RJSE	RDR	LRLE	LRPP_GRR	FSP	LRAGE	NGLGE	
EYaleB	10	50.02 \pm 1.90	57.86 \pm 1.02	43.07 \pm 1.27	83.19 \pm 0.97	61.74 \pm 1.83	45.76 \pm 1.27	54.05 \pm 1.65	50.54 \pm 1.28	85.45 \pm 0.93	81.20 \pm 1.32	39.39 \pm 1.99	85.91\pm0.93	
	15	58.75 \pm 2.29	64.44 \pm 1.67	52.55 \pm 0.81	87.35 \pm 0.51	68.83 \pm 4.22	54.34 \pm 0.88	59.44 \pm 2.25	56.04 \pm 2.05	90.27\pm0.62	85.56 \pm 0.40	53.02 \pm 4.19	89.64 \pm 0.57	
	20	64.88 \pm 1.63	68.96 \pm 0.61	58.72 \pm 0.82	89.14 \pm 0.92	75.62 \pm 0.92	60.21 \pm 1.00	63.31 \pm 1.32	60.60 \pm 1.27	91.44\pm0.59	86.63 \pm 1.11	61.14 \pm 3.67	91.22 \pm 0.80	
YTC	25	67.96 \pm 1.62	72.64 \pm 1.26	62.23 \pm 1.10	89.99 \pm 0.89	78.33 \pm 0.86	63.48 \pm 0.94	65.48 \pm 0.99	63.31 \pm 0.95	92.11 \pm 0.65	88.29 \pm 0.96	67.81 \pm 3.59	92.38\pm0.41	
	10	70.79 \pm 0.89	71.98 \pm 0.99	76.04 \pm 1.03	66.86 \pm 0.86	72.77 \pm 1.07	76.18 \pm 1.05	76.09 \pm 0.95	75.67 \pm 0.98	76.99\pm1.08	72.39 \pm 0.92	75.30 \pm 1.06	76.27 \pm 1.03	
	15	79.29 \pm 0.96	79.84 \pm 0.80	82.37 \pm 0.86	75.60 \pm 0.83	79.31 \pm 0.92	82.43 \pm 0.79	82.50 \pm 0.78	81.84 \pm 0.82	82.54\pm0.75	79.26 \pm 1.22	81.17 \pm 0.92	82.50 \pm 0.81	
Binalpha	20	83.14 \pm 0.67	84.16 \pm 0.75	85.48 \pm 0.59	80.19 \pm 0.45	82.83 \pm 0.55	85.49 \pm 0.60	85.39 \pm 0.59	84.91 \pm 0.62	84.88 \pm 0.51	82.63 \pm 0.81	84.36 \pm 0.90	85.59\pm0.61	
	25	85.82 \pm 0.48	86.83 \pm 0.41	87.75 \pm 0.54	83.24 \pm 0.60	85.44 \pm 0.67	87.75 \pm 0.56	87.67 \pm 0.52	87.12 \pm 0.47	86.62 \pm 0.53	84.81 \pm 0.51	86.65 \pm 0.65	87.83\pm0.54	
	10	38.31 \pm 1.52	39.25 \pm 1.56	60.60 \pm 1.67	17.13 \pm 1.17	57.99 \pm 1.91	60.21 \pm 1.87	60.30 \pm 1.77	60.11 \pm 1.85	49.12 \pm 4.32	24.54 \pm 2.85	60.58 \pm 1.75	61.84\pm1.49	
USPS	15	54.27 \pm 1.56	55.54 \pm 1.81	64.69 \pm 1.46	25.57 \pm 1.59	62.37 \pm 1.10	64.48 \pm 1.05	64.73 \pm 1.16	64.09 \pm 1.47	54.54 \pm 2.25	27.09 \pm 3.65	64.02 \pm 1.65	65.50\pm0.97	
	20	60.53 \pm 2.32	61.86 \pm 1.48	67.06 \pm 1.29	30.91 \pm 2.02	62.68 \pm 2.48	66.61 \pm 1.29	66.65 \pm 1.00	67.19 \pm 1.42	55.92 \pm 3.45	26.71 \pm 1.69	66.56 \pm 1.67	68.11\pm0.98	
	30	85.61 \pm 0.61	86.12 \pm 0.76	86.40 \pm 0.77	83.28 \pm 1.55	86.44 \pm 0.91	86.31 \pm 0.91	89.58 \pm 0.61	90.23 \pm 0.29	88.68 \pm 0.55	89.12 \pm 0.54	87.52 \pm 0.64	82.70 \pm 1.06	89.57 \pm 0.41
ETH80	40	90.29 \pm 0.41	90.78 \pm 0.45	90.36 \pm 0.53	87.69 \pm 0.56	90.88 \pm 0.99	91.23 \pm 0.40	90.25 \pm 0.41	90.58 \pm 0.32	89.69 \pm 0.60	84.31 \pm 1.18	90.71 \pm 0.35	91.28\pm0.40	
	10	49.11 \pm 1.42	49.65 \pm 1.73	58.27 \pm 1.19	58.56 \pm 1.20	36.77 \pm 2.35	57.97 \pm 1.72	59.13 \pm 1.55	59.47\pm1.56	51.35 \pm 3.76	46.65 \pm 1.89	58.53 \pm 1.34	58.71 \pm 1.24	
	20	29.20 \pm 3.56	28.32 \pm 3.21	53.84 \pm 1.38	64.68 \pm 1.28	40.59 \pm 1.76	63.69 \pm 1.43	64.58 \pm 0.82	64.59 \pm 0.69	58.80 \pm 2.59	30.21 \pm 1.17	63.07 \pm 1.55	65.19\pm1.16	
15-Scene	30	57.86 \pm 1.17	62.49 \pm 0.71	61.14 \pm 1.06	68.40 \pm 0.69	46.46 \pm 1.06	67.40 \pm 0.58	67.32 \pm 1.05	67.07 \pm 1.11	62.79 \pm 1.30	36.95 \pm 1.32	66.60 \pm 0.59	68.98\pm0.95	
	40	65.94 \pm 1.13	68.20 \pm 1.13	66.28 \pm 1.08	70.94 \pm 0.99	51.51 \pm 3.12	70.09 \pm 1.04	70.54 \pm 1.15	69.75 \pm 1.18	67.07 \pm 1.14	40.71 \pm 0.97	68.78 \pm 1.02	71.66\pm1.19	
	10	80.96 \pm 1.89	82.49 \pm 1.31	89.14 \pm 0.86	88.74 \pm 1.01	84.85 \pm 2.26	89.67 \pm 0.92	89.68 \pm 0.85	88.46 \pm 1.09	86.38 \pm 0.85	86.86 \pm 1.31	89.40 \pm 0.85	90.13\pm1.02	
USPS	20	90.05 \pm 1.16	87.20 \pm 1.04	93.05 \pm 0.71	92.60 \pm 0.67	89.57 \pm 1.47	92.76 \pm 0.73	93.36 \pm 0.69	92.43 \pm 0.75	90.69 \pm 1.17	77.45 \pm 0.99	93.32 \pm 0.75	93.91\pm0.74	
	30	94.07 \pm 0.64	90.86 \pm 0.65	94.98 \pm 0.52	94.06 \pm 0.44	92.39 \pm 0.62	94.52 \pm 0.45	94.97 \pm 0.46	94.36 \pm 0.56	93.01 \pm 0.61	81.89 \pm 1.26	95.08 \pm 0.41	95.59\pm0.39	
	40	95.00 \pm 0.32	92.06 \pm 0.32	95.52 \pm 0.35	94.60 \pm 0.29	93.21 \pm 0.50	95.00 \pm 0.26	95.55 \pm 0.33	95.14 \pm 0.31	93.80 \pm 0.52	85.63 \pm 0.97	95.68 \pm 0.33	96.06\pm0.29	

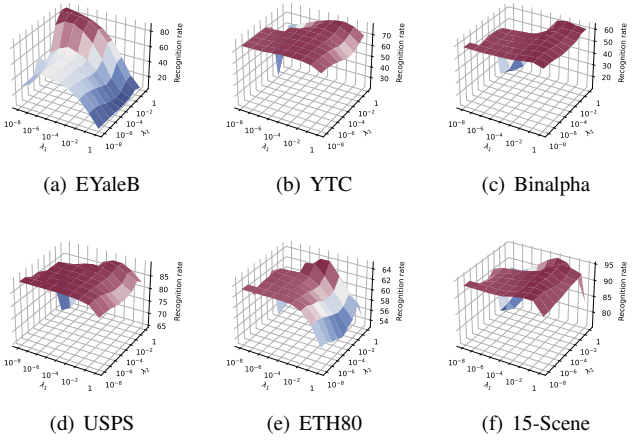


Fig. 1. Recognition rate versus the parameters λ_1 and λ_2 on six databases with training samples of 10, 10, 10, 20, 20 and 20 per category respectively.

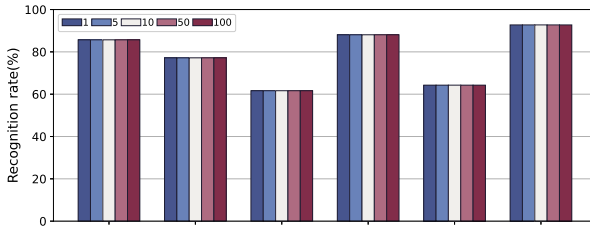


Fig. 2. Classification performance (%) versus hyper-parameter λ_3 on six different databases with 10, 10, 10, 20, 20 and 20 training samples per class, respectively.

parameters. As a result, we determine λ_3 values independently. However, λ_1 and λ_2 exhibit interdependence, leading us to perform a grid search to identify optimal values for these two parameters. Specifically, λ_1 and λ_2 are selected from $\{10^{-8}, 10^{-7}, 10^{-6}, 10^{-5}, 10^{-4}, 10^{-3}, 10^{-2}, 0.1, 1\}$ and λ_3 is chosen from $\{1, 5, 10, 50, 100\}$. Fig. 1 illustrates the performance of the proposed algorithm under different parameters combining across six databases. By fixing other

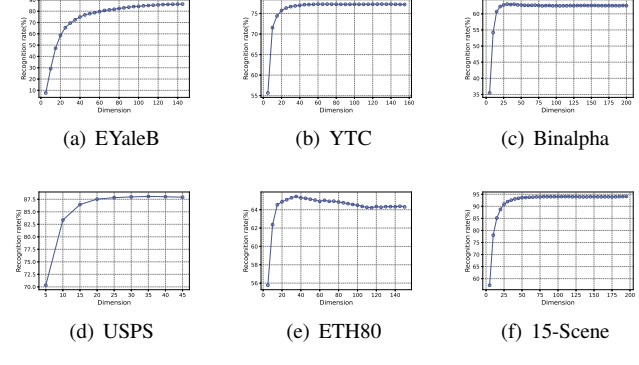


Fig. 3. Recognition rate versus the reduced dimension on six databases with training samples of 10, 10, 10, 20, 20 and 20 per category respectively.

hyper-parameters, we show the impact of different λ_3 on classification performance in Fig. 2, which verifies that our model is insensitive to the selection of λ_3 in its candidate set.

E. Research on dimensionality sensitivity

To conduct feature extraction, we assessed the proposed method at various dimensionalities on six distinct databases respectively. Fig. 3 depicts the recognition rate versus reduced dimension. From the figure, we can observe that the model delivers satisfactory performance across a broad range of feature dimensions, provided that the dimensionality is not excessively low. In our reported results, we employed reduced dimensions of 140, 150, 200, 40, 70 and 140 for all methods on EYaleB, YTC, Binalpha, USPS, ETH80 and 15-Scene databases, respectively.

F. Convergence study

In this section, we establish the convergence property of our approach from an experimental perspective, conducting six experiments on the EYaleB, YTC, Binalpha, USPS, ETH80 and 15-Scene databases. Fig. 4 shows the objective value and constraint error versus different iterations for the six databases. The plots demonstrate that the objective loss and

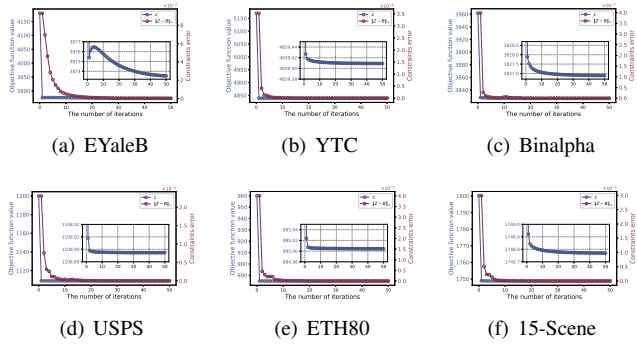


Fig. 4. Convergence curves of our method on six databases with training samples of 10, 10, 10, 20, 20 and 20 per category respectively.

constraints error of our learning model (7) steadily decrease and eventually stabilize, indicating that the exploited optimization algorithm exhibits favorable convergence properties.

V. CONCLUSION

In summary, this paper introduces a generalized linear graph embedding method. Firstly, we propose a neighborhood-adaptive graph learning approach that does not require pre-defining the neighborhood size. Secondly, the diversity in mining latent patterns is determined by the low-rank representation and the $\ell_{2,0}$ column sparsity of the projection matrix. Experimental results demonstrate the outstanding performance of the proposed method in handling various scenarios.

REFERENCES

- [1] H. Cai, V. W. Zheng, and K. C.-C. Chang, "A comprehensive survey of graph embedding: Problems, techniques, and applications," *IEEE Transactions on Knowledge and Data Engineering*, vol. 30, no. 9, pp. 1616–1637, 2018.
- [2] X. Wang, D. Bo, C. Shi, S. Fan, Y. Ye, and S. Y. Philip, "A survey on heterogeneous graph embedding: methods, techniques, applications and sources," *IEEE Transactions on Big Data*, vol. 9, no. 2, pp. 415–436, 2022.
- [3] X. Lu, J. Long, J. Wen, L. Fei, B. Zhang, and Y. Xu, "Locality preserving projection with symmetric graph embedding for unsupervised dimensionality reduction," *Pattern Recognition*, vol. 131, p. 108844, 2022. [Online]. Available: <https://www.sciencedirect.com/science/article/pii/S0031320322003259>
- [4] L. Jiang, X. Fang, W. Sun, N. Han, and S. Teng, "Low-rank constraint based dual projections learning for dimensionality reduction," *Signal Processing*, vol. 204, p. 108817, 2023. [Online]. Available: <https://www.sciencedirect.com/science/article/pii/S0165168422003565>
- [5] X. He, S. Yan, Y. Hu, P. Niyogi, and H.-J. Zhang, "Face recognition using laplacianfaces," *IEEE Transactions on Pattern Analysis and Machine Intelligence*, vol. 27, no. 3, pp. 328–340, 2005.
- [6] D. Cai, X. He, J. Han, and H.-J. Zhang, "Orthogonal laplacianfaces for face recognition," *IEEE Transactions on Image Processing*, vol. 15, no. 11, pp. 3608–3614, 2006.
- [7] R. Wang, F. Nie, R. Hong, X. Chang, X. Yang, and W. Yu, "Fast and orthogonal locality preserving projections for dimensionality reduction," *IEEE Transactions on Image Processing*, vol. 26, no. 10, pp. 5019–5030, 2017.
- [8] H. Chen, F. Nie, R. Wang, and X. Li, "Adaptive flexible optimal graph for unsupervised dimensionality reduction," *IEEE Signal Processing Letters*, vol. 28, pp. 2162–2166, 2021.
- [9] J. Wen, N. Han, X. Fang, L. Fei, K. Yan, and S. Zhan, "Low-rank preserving projection via graph regularized reconstruction," *IEEE Transactions on Cybernetics*, vol. 49, no. 4, pp. 1279–1291, 2019.
- [10] L. Hu, Z. Dai, L. Tian, and W. Zhang, "Class-oriented self-learning graph embedding for image compact representation," *IEEE Transactions on Circuits and Systems for Video Technology*, vol. 33, no. 1, pp. 74–87, 2023.
- [11] F. Nie, X. Wang, and H. Huang, "Clustering and projected clustering with adaptive neighbors," in *Proceedings of the 20th ACM SIGKDD International Conference on Knowledge Discovery and Data Mining*, ser. KDD '14. New York, NY, USA: Association for Computing Machinery, 2014, p. 977–986. [Online]. Available: <https://doi.org/10.1145/2623330.2623726>
- [12] W. Wang, Y. Yan, F. Nie, S. Yan, and N. Sebe, "Flexible manifold learning with optimal graph for image and video representation," *IEEE Transactions on Image Processing*, vol. 27, no. 6, pp. 2664–2675, 2018.
- [13] Y. Pang, B. Zhou, and F. Nie, "Simultaneously learning neighborhood and projection matrix for supervised dimensionality reduction," *IEEE Transactions on Neural Networks and Learning Systems*, vol. 30, no. 9, pp. 2779–2793, 2019.
- [14] F. Nie, Z. Wang, R. Wang, Z. Wang, and X. Li, "Adaptive local linear discriminant analysis," *ACM Trans. Knowl. Discov. Data*, vol. 14, no. 1, feb 2020. [Online]. Available: <https://doi.org/10.1145/3369870>
- [15] X. Li, Q. Wang, F. Nie, and M. Chen, "Locality adaptive discriminant analysis framework," *IEEE Transactions on Cybernetics*, vol. 52, no. 8, pp. 7291–7302, 2022.
- [16] L. Hu, W. Zhang, and Z. Dai, "Joint sparse locality-aware regression for robust discriminative learning," *IEEE Transactions on Cybernetics*, vol. 52, no. 11, pp. 12 245–12 258, 2022.
- [17] Y. Lu, Z. Lai, Y. Xu, X. Li, D. Zhang, and C. Yuan, "Low-rank preserving projections," *IEEE transactions on cybernetics*, vol. 46, no. 8, pp. 1900–1913, 2015.
- [18] Y. Yi, J. Wang, W. Zhou, Y. Fang, J. Kong, and Y. Lu, "Joint graph optimization and projection learning for dimensionality reduction," *Pattern Recognition*, vol. 92, pp. 258–273, 2019.
- [19] Z. Lai, J. Bao, H. Kong, M. Wan, and G. Yang, "Discriminative low-rank projection for robust subspace learning," *International Journal of Machine Learning and Cybernetics*, vol. 11, pp. 2247–2260, 2020.
- [20] Z. Huang, S. Zhao, L. Fei, and J. Wu, "Weighted graph embedded low-rank projection learning for feature extraction," in *ICASSP 2022 - 2022 IEEE International Conference on Acoustics, Speech and Signal Processing (ICASSP)*, 2022, pp. 1501–1505.
- [21] M. Cai, X. Shen, S. E. Abdiomien, Y. Cai, and S. Tian, "Robust dimensionality reduction via low-rank laplacian graph learning," *ACM Trans. Intell. Syst. Technol.*, vol. 14, no. 3, 2023.
- [22] T. Zhang, C.-F. Long, Y.-J. Deng, W.-Y. Wang, S.-Q. Tan, and H.-C. Li, "Low-rank preserving embedding regression for robust image feature extraction," *IET Computer Vision*, vol. 18, no. 1, pp. 124–140, 2024.
- [23] G. Liu, Z. Lin, S. Yan, J. Sun, Y. Yu, and Y. Ma, "Robust recovery of subspace structures by low-rank representation," *IEEE Transactions on Pattern Analysis and Machine Intelligence*, vol. 35, no. 1, pp. 171–184, 2013.
- [24] G. Liu and S. Yan, "Latent low-rank representation for subspace segmentation and feature extraction," in *2011 International Conference on Computer Vision*, 2011, pp. 1615–1622.
- [25] M. Yin, S. Cai, and J. Gao, "Robust face recognition via double low-rank matrix recovery for feature extraction," in *2013 IEEE International Conference on Image Processing*, 2013, pp. 3770–3774.
- [26] W. K. Wong, Z. Lai, J. Wen, X. Fang, and Y. Lu, "Low-rank embedding for robust image feature extraction," *IEEE Transactions on Image Processing*, vol. 26, no. 6, pp. 2905–2917, 2017.
- [27] X. Fang, N. Han, J. Wu, Y. Xu, J. Yang, W. K. Wong, and X. Li, "Approximate low-rank projection learning for feature extraction," *IEEE Transactions on Neural Networks and Learning Systems*, vol. 29, no. 11, pp. 5228–5241, 2018.
- [28] Z. Ren, Q. Sun, B. Wu, X. Zhang, and W. Yan, "Learning latent low-rank and sparse embedding for robust image feature extraction," *IEEE Transactions on Image Processing*, vol. 29, pp. 2094–2107, 2020.
- [29] Y. Zhang, M. Xiang, and B. Yang, "Low-rank preserving embedding," *Pattern Recognition*, vol. 70, pp. 112–125, 2017.
- [30] Y. Chen, Z. Lai, W. K. Wong, L. Shen, and Q. Hu, "Low-rank linear embedding for image recognition," *IEEE Transactions on Multimedia*, vol. 20, no. 12, pp. 3212–3222, 2018.
- [31] T. Pang, F. Nie, J. Han, and X. Li, "Efficient feature selection via $\ell_{2,0}$ -norm constrained sparse regression," *IEEE Transactions on Knowledge and Data Engineering*, vol. 31, no. 5, pp. 880–893, 2019.
- [32] S. Boyd, N. Parikh, E. Chu, B. Peleato, and J. Eckstein, "Distributed optimization and statistical learning via the alternating direction method of multipliers," *Foundations and Trends® in Machine Learning*, vol. 3, no. 1, pp. 1–122, 2011. [Online]. Available: <http://dx.doi.org/10.1561/2200000016>
- [33] M. Hong, Z.-Q. Luo, and M. Razaviyayn, "Convergence analysis of alternating direction method of multipliers for a family of nonconvex

problems," *SIAM Journal on Optimization*, vol. 26, no. 1, pp. 337–364, 2016. [Online]. Available: <https://doi.org/10.1137/140990309>

[34] P. Zhu, X. Hou, K. Tang, Y. Liu, Y.-P. Zhao, and Z. Wang, "Unsupervised feature selection through combining graph learning and $\ell_{2,0}$ -norm constraint," *Information Sciences*, vol. 622, pp. 68–82, 2023.

[35] H. Zou, T. Hastie, and R. Tibshirani, "Sparse principal component analysis," *Journal of Computational and Graphical Statistics*, vol. 15, no. 2, pp. 265–286, 2006.

[36] S. P. Boyd and L. Vandenberghe, *Convex optimization*. Cambridge university press, 2004.

[37] X. He, D. Cai, S. Yan, and H.-J. Zhang, "Neighborhood preserving embedding," in *Tenth IEEE International Conference on Computer Vision (ICCV'05) Volume 1*, vol. 2, 2005, pp. 1208–1213 Vol. 2.

[38] F. Nie, W. Zhu, and X. Li, "Unsupervised feature selection with structured graph optimization," in *Proceedings of the Thirtieth AAAI Conference on Artificial Intelligence*, ser. AAAI'16. AAAI Press, 2016, p. 1302–1308.

[39] Z. Lai, Y. Chen, D. Mo, J. Wen, and H. Kong, "Robust jointly sparse embedding for dimensionality reduction," *Neurocomputing*, vol. 314, pp. 30–38, 2018. [Online]. Available: <https://www.sciencedirect.com/science/article/pii/S0925231218307872>

[40] Z. Lai, D. Mo, W. K. Wong, Y. Xu, D. Miao, and D. Zhang, "Robust discriminant regression for feature extraction," *IEEE Transactions on Cybernetics*, vol. 48, no. 8, pp. 2472–2484, 2018.

[41] C. Tang, X. Liu, X. Zhu, J. Xiong, M. Li, J. Xia, X. Wang, and L. Wang, "Feature selective projection with low-rank embedding and dual laplacian regularization," *IEEE Transactions on Knowledge and Data Engineering*, vol. 32, no. 9, pp. 1747–1760, 2020.

[42] J. Lu, H. Wang, J. Zhou, Y. Chen, Z. Lai, and Q. Hu, "Low-rank adaptive graph embedding for unsupervised feature extraction," *Pattern Recognition*, vol. 113, p. 107758, 2021. [Online]. Available: <https://www.sciencedirect.com/science/article/pii/S0031320320305616>

[43] A. Georghiades, P. Belhumeur, and D. Kriegman, "From few to many: illumination cone models for face recognition under variable lighting and pose," *IEEE Transactions on Pattern Analysis and Machine Intelligence*, vol. 23, no. 6, pp. 643–660, 2001.

[44] L. Wolf, T. Hassner, and I. Maoz, "Face recognition in unconstrained videos with matched background similarity," in *CVPR 2011*, 2011, pp. 529–534.

[45] J. Hull, "A database for handwritten text recognition research," *IEEE Transactions on Pattern Analysis and Machine Intelligence*, vol. 16, no. 5, pp. 550–554, 1994.

[46] B. Leibe and B. Schiele, "Analyzing appearance and contour based methods for object categorization," in *2003 IEEE Computer Society Conference on Computer Vision and Pattern Recognition, 2003. Proceedings.*, vol. 2, 2003, pp. II–409.

[47] S. Lazebnik, C. Schmid, and J. Ponce, "Beyond bags of features: Spatial pyramid matching for recognizing natural scene categories," in *2006 IEEE Computer Society Conference on Computer Vision and Pattern Recognition (CVPR'06)*, vol. 2, 2006, pp. 2169–2178.

[48] Z. Jiang, Z. Lin, and L. S. Davis, "Label consistent k-svd: Learning a discriminative dictionary for recognition," *IEEE Transactions on Pattern Analysis and Machine Intelligence*, vol. 35, no. 11, pp. 2651–2664, 2013.